STRUCTURAL AND SPECTRAL STUDIES OF SUNSPOTS

Grant NGR-39-005-066
Supplement No. 2

NATIONAL AERONAUTICS AND SPACE ADMINISTRATION

Annual Report

Period: September 1, 1969 - August 31, 1970

Principal Investigator: Arne A. Wyller

Bartol Research Foundation
of
The Franklin Institute
Swarthmore, Pennsylvania
19081

Submitted: September 17, 1970

I. Observational Results

In the course of the past year a vigorous observing program has been initiated on sunspot photoelectric line profiles for some of the major Fraunhofer lines such as H-alpha, Na D_2 and CaI λ4227. Recently we have been able to add to our scan "collection" infrared recordings of the HeIλ10,830 line with our new infrared photomultiplier.

Particular attention was paid to the big spot groups which developed October 18-26 and reappeared in the latter half of November. On both occasions, pressure scans of these lines were made for selected spots with the echelle alone at a resolution of 0.10 - 0.15 A. Since the theoretical interests center on the precise shape of the broad line wings this resolution appeared accurate enough.

During these recordings a whole new realm of experience has opened up with our instrument and we have felt greatly encouraged by our results to have confidence in our new scan technique. While originally our intention by scanning the profiles of the broad major Fraunhofer lines was merely to gain experience in operational procedures with our instrument, we have become increasingly aware of the fact that virtually no photoelectric recordings of line profiles exist of <u>any</u> sunspot lines, although a few such recordings do exist for disk lines (Pierce 1954, David 1961). All work on sunspot line profiles has hitherto concentrated exclusively on photographic methods. Such techniques are very seriously hampered by the fundamental problem of eliminating scattered photospheric light caused by inadequate guiding of the telescope and seeing fluctuations.

Many ingenious reduction techniques have evolved to solve this photographic problem. According to Zwaan's thorough critique of these procedures none are truly satisfactory (Zwaan 1965a). It thus appears quite desirable to evolve a new technique of intensity recording to calibrate the best photographic results and if possible to improve upon them. We believe that during this past year the development of our particular instrumental combination and operational procedure has led to such a new technique.

The observational procedure that we have adopted on the basis of our experiences this fall is briefly as follows: from the observed size of the spot, using the area-temperature relation of Elste (Elste 1967) we calculate the expected continuum intensity ratio of the spot and the photosphere as a function of wavelength and position on the disk at the time of observation (see Figures 2, 3 and 4). This intensity ratio serves as a rough quality criterion for the guiding accuracy on the spot and the seeing fluctuations. For a given wavelength we record in both continuum and line channels first the dark current, then the intensity of the solar disk center and finally the spot intensity with pulsecounting integration times of 0.8 seconds and print-out on paper tape. Typically some 50 "time channels", each of 0.8 seconds duration will be printed out. Most of these spot continuum samplings will show the effects of photospheric light contamination caused by improper guiding and seeing fluctuations, but a few will show count rates near the expected value from the predicted spot-disk continuum intensity ratios. These "time channels" we accept as representative spot line profile samplings with minimal photospheric light contamination. Typically at H-alpha we have had ratios of 0.27 - 0.28 as the acceptance criterion for spots 12-15 seconds of arc in umbral diameters. Further umbral continuum observations on larger spots (20" umbral diameter) gives values in the blue and yellow spectral regions in good agreement with the careful photographic observations of Wittman and Schröter (1969).

The great advantage of this photoelectric recording technique is that one at any stage can interrupt the pulse count recordings and wait for moments of good seeing to record some "clean" spot samplings, while in conventional photography one has had to record continuously and accept good and bad seeing moments intermixed. Our observations were done under generally poor seeing conditions. In effect we are carrying out spectroscopically what Bray and Loughhead have been doing in white light photography of sunspots, where they trigger exposures by a seeing monitor. In fact they suggest building up exposures of photographic spectrograms by intermittent exposures in the same way (Bray and Loughhead 1965) that we are doing photoelectrically. Our integration times are a little long, 0.8 seconds, but gating our pulsecounters for 0.1 second integration times we do not observe our relative spot count ratios to go further down. We believe from the recent study by Brandt (1969) that our present integration times are short enough to freeze image motion acceptably.

Having evolved a technique which we feel significantly reduces the scattered light levels in the blurring effect of the photosphere, there remains the effects of scattered light in the instrument and in the terrestrial atmosphere. We have in the operational sequence of measurements for a given wavelength included also measurements of the sky brightness at various distances outside of the solar limb. We have been agreeably surprised at the low levels of total scattered light (instrumental and atmospheric) that we record. On an average clear day these sources of light scattering amount to one percent or less at a distance of 30 seconds of arc from the solar limb (see Figure 1). We have adopted the rule of thumb of Zwaan (1965b) based on the theoretical work of David and Elste (1962) to multiply by a factor of 4 the count rate 1 minute of arc outside the solar limb, to arrive at the scattered light level on the solar disk center. By recording the scattered light both in the continuum channel and the line channel over all wavelengths in the scanned profile, we have ascertained that the sky scattered light is photospheric in origin, judging from the deep central intensity of H-alpha in the scattered light profile.

We thus believe on the basis of our observational experience this fall and winter that our new observational technique will yield sunspot line profiles accurate to a few percent. Some sample scans are shown in Figures 5, 6 and 7 together with theoretical profiles calculated by our new post-doctoral research fellow, Dr. Hong-Sik Yun. The significance of these will be described in the next section, but we note here in Figure 10 the good agreement in the NaD_2 line profile between our photoelectric observations and the photographic ones by Baranovsky and Stepanov (1959) for a similar sized spot.

The infrared line observations have centered on the neutral helium line at λ10,830. Two line profiles are reproduced in Figure 8. There is an apparent enhancement in the line strength over the umbra as compared to the disk, which is contrary to the expectations on the basis of a cooler umbral chromosphere. We have suspected plage contamination overlying these particular spot umbrae. However, none show up overlying these umbrae in H-alpha photography, kindly sent us by Dr. Howard of the Hale Observatories. At the suggestion of Dr. Zirin, to whom we forwarded these results, we contacted in May, Dr. Mallia, in charge of the field station in Switzerland for the Oxford solar spectral scanner. He kindly made a scan on June 6 of the HeI 10,830 line, which also shows a strengthening over the spot umbra. On the other hand in extensive discussions with Drs. Harvey and Hull at the recent IAU meeting in Brighton, they report that their Kitt Peak 10,830 spectroheliograms do _not_ show enhanced absorption over spot umbra. Obviously, more observations are needed - and are merited - in view of the important consequences for the physics of the umbral chromosphere. If our observed strengthening of the line is conclusively verified, this could be interpreted as an effect of preferential energy dumping in the umbral chromosphere by hydromagnetic mechanisms, which are enhanced by the strong magnetic fields in the umbra.

Other circumstantial evidence for umbral chromosphere heating lie in the observations that the H-alpha line core does not disappear over spot umbrae (see Figure 5) and our recent observations that the umbral residual central intensity of the NaD_2 line is slightly lower than in the disk (about 3% as against 5%).

Finally, in this section, we would like to point out that our photoelectric recording technique in principle should enable us to build up also penumbral line profiles which are of great interest to study with model atmosphere calculations. The selection criterion for the appropriate time channels would then be increased to a value of 0.7 - 0.8 in the continuum intensity ratio of spot to disk. While our present umbral line profiles carry information on the temperature and pressure gradients along the magnetic field radially outward, the penumbral line profiles probe the atmospheric conditions where the field lines are almost tangential to the solar surface. It is to be expected there that a magnetic pressure component will enter in and modify the hydrostatic pressure gradients of the penumbral atmosphere. Thus a study of penumbral line profiles is of the greatest theoretical interest and we hope to pursue this in the coming research period.

II. Theoretical Studies of Sunspots

Yun extended the atmospheres of his magnetostatic models of sunspots (1968) up to a monochromatic optical depth at 5000Å, $\tau_o=10^{-3}$, using the scaled empirical solar T-τ_o relation proposed by Krishna Swamy (1967). Also he applied the magneto-static theory of sunspots by Schlüter and Temesvary (1958) to calculate the strength of the magnetic field on the axis of symmetry for these spots. In the calculations the chemical compositions and the surface gravity in the spots were taken to be identical to those of the normal photosphere. In computing these models four values of effective temperature corresponding to 4000, 4400, 4600 and 5000°K were considered.

Assuming the condition of local thermodynamic equilibrium, Yun computed monochromatic emergent intensity of these spots as a function of μ ($\mu=\cos\theta$, where θ is the heliocentric angle). In order to investigate the limb darkening laws for these spots, the computed intensity $I_\lambda^*(\mu)$ of each spot was normalized by that of the normal photosphere $I_\lambda^\odot(1)$ at the disk center. In particular, the intensity ratio, $I_\lambda^*(\mu)/I_\lambda^\odot(1)$ computed at the following selected wavelengths, 4230Å, 5900Å and 6560Å are presented in Figures 2, 3 and 4 (where the expected size of the umbra of each average observed spot is indicated beside its corresponding effective temperature). The expected umbral size of the average observed spots was obtained from the statistical relation between the effective temperature and the umbral area given by Elste (1967).

As can be seen from the figues, the intensity ratio $I_\lambda^*(\mu)/I_\lambda^\odot(1)$ is quite sensitive to the effective temperature of the spots. It is, therefore, an important quantity in determining the effective temperature of sunspots from observations. With the aid of our present pressure scanner, Wyller and Fay carried out sunspot observations at the Flower and Cook Observatory of the University of Pennsylvania. Three small sized spots (i.e., the umbral diameter is less than about 10 seconds of arc) were observed during the months of January and February. The measured intensity ratios for these spots are plotted in Figs. 2, 3 and 4 (see open circle and triangle). It is interesting to note that the temperature determined from the intensity measurements agrees well with the estimated temperature from the size of the umbra given by Elste's statistical relation (between the effective temperature and the umbral area).

Yun further extended his investigation of sunspots by studying spectral line formation in the spots. He computed profiles of strong lines such as H_α, NaI D_2, CaI 4227 and MgI 5184, utilizing his sunspot models. In his calculation it was assumed that the lines are formed by pure absorption except in the immediate neighborhood of the line center. In computing profiles, radiation damping and collisional damping were considered. For the calculation of the collisional damping constant the collisions of the radiating atom with neutral hydrogen atoms, neutral helium atoms and electrons were taken into account. In particular, when the profile of H_α was computed, the Stark effect caused by collisions with ions and electrons and resonance broadening were included. Yun used Griem's theory of Stark broadening of hydrogen. The addition of combined Doppler, natural, collisional broadening to Stark broadening has been done by a convolution of the two types of the profiles. The abundance of the elements considered in the present calculation were taken from the solar abundance by Goldberg, Muller and Aller (1960). The computed profiles of H_α, NaI D_2 and CaI 4227 are shown in Figs. 4, 5 and 6 respectively, and they are compared with the profiles observed by Wyller and Fay. The result of the comparison shows that the agreement between the observed and computed profiles is fairly good, indicating that the umbral atmospheres can be well explained by a model atmosphere in radiative equilibrium for the small sized sunspots. The present preliminary investigation seems to support the supposition of the hydrostatic equilibrium in the umbra of spots, noting that Yun's models (i.e., umbral models) have been constructed on the basis of the hydrostatic equilibrium. The validity of the hydrostatic equilibrium in sunspot umbra is still in debate among investigators.

An even more extensive study has been made by looking into the center-to-limb variation of the umbral continuous intensity as well as the profile of the strong Na D_2 line. To our surprise, for large sunspots, a considerable disagreement has been found between the observed and calculated profiles based on a radiative equilibrium sunspot model as shown in Figure 10b. In addition, the umbral continuum intensity for the large spot relative to that of the normal adjacent photosphere is shown to increase with the heliocentric angle, θ, as also found by other workers such as Rödberg (1966), Mattig (1969) and Wittmann and Schröter (1969) from their photographic observations.

An attempt, therefore, has been made to derive a new relationship between temperature T and optical depth τ_0 at 5000Å, which can reproduce the recent observations of the center-to-limb variation of the umbral intensity as closely as possible. The present investigation employs the infrared observations of Wittmann and Schröter (1969) along with our own observations to calculate the temperature distribution of a large umbra, assuming the condition of local thermodynamic equilibrium (LTE). Since limb darkening observations cannot yield reliable information on the temperature structure at optical depths larger than unity, the present study utilizes Yun's internal model (1968) to represent such deep regions of the atmospheres. Table I presents the resulting temperature distribution as a function of optical depth τ_o. Making use of the new T - τ_o relation the gas pressure, P_g is calculated, assuming that the umbra is in hydrostatic equilibrium. This empirical T - τ_o relation is compared with other proposed empirical models of umbrae (e.g., Makita (1963), Zwaan (1965), Branch (1969), Henoux (1969) and Wittmann and Schröter (1969)) in Figure 10a.

Our proposed model predicts not only the recent limb darkening observations in various wavelength regions but also the profile of the violet wing of the Na D_2 line observed in the spectrum of our large sunspot (Au$\simeq$100). The results are demonstrated in Figure 9 and Figure 10b, where the profile of Na D_2 line and the emergent intensities have been computed under the assumption of LTE with H, H^- and electron scattering being the source of continuous opacity. It is noticeable from Figure 9 that the scaled solar model of T^*_{eff}=4000^{o}K and the models derived by Makita (1963) and Zwaan (1965) (which are basically radiative equilibrium models) fail to show any "limb-brightening" effect. The agreement between the computed value of our model and Henoux's measurement (1968) near 16000Å shows that there is a steep rise in temperature gradient in greater depths ($\tau_o \gtrsim 1$) as found in our proposed model.

Table I. A New Empirical Umbral Model ($A_u \simeq 100$)

$\log \tau_o$	$T(^oK)$	$\log P_g$	$\kappa_{5000}(cm^2/gr)$	$P_e(dyne/cm^2)$
-3.0	3360	3.85	7.40(-3)	4.36(-2)
-2.8	3375	3.96	8.96(-3)	5.41(-2)
-2.6	3390	4.06	1.09(-2)	6.72(-2)
-2.4	3410	4.17	1.33(-2)	8.45(-2)
-2.2	3461	4.28	1.65(-2)	1.13(-1)
-2.0	3579	4.39	2.12(-2)	1.71(-1)
-1.8	3680	4.50	2.71(-2)	2.50(-1)
-1.6	3770	4.60	3.43(-2)	3.56(-1)
-1.4	3840	4.70	4.27(-2)	4.85(-1)
-1.2	3900	4.80	5.29(-2)	6.46(-1)
-1.0	3950	4.91	6.49(-2)	8.41(-1)
-0.8	3980	5.01	7.85(-2)	1.05
-0.6	4010	5.12	9.53(-2)	1.33
-0.4	4051	5.23	1.17(-1)	1.70
-0.2	4109	5.34	1.45(-1)	2.26
0.0	4150	5.45	1.77(-1)	2.89
0.2	4221	5.56	2.22(-1)	3.90
0.4	4405	5.66	2.99(-1)	6.36
0.6	4750	5.76	4.27(-1)	1.26(+1)
0.8	5160	5.85	5.79(-1)	2.43(+1)
1.0	5700	5.93	8.29(-1)	5.20(+1)

The atmosphere of large umbrae consist of two distinctly different regions, one upper region with extremely small temperature gradient (almost isothermal) in the range of $0.04 \lesssim \tau_0 \lesssim 1$ and a deeper zone beyond $\tau_0 \simeq 1$ with fairly high temperature gradient. The departure from radiative equilibrium appears to be well established with acceptance of the assumption of hydrostatic equilibrium. The existence of the extremely small temperature gradient with consequent departure from radiative equilibrium may be attributed to heating created by the lateral influx of radiation into the umbra from the penumbra and the normal photosphere as discussed by Zwaan (1965) and Fullerton and Elste (1969).

III. Instrumental Developments

a) Microwave Discharge Tubes

Since our instrument can achieve a resolution of 0.01A, we need precise laboratory wavelength standards of each spectral line of each element we observe in the solar spectrum. The standard wavelength sources must have very narrow spectral lines hence the need of the temperature of the atoms emitting be less than 1000°K. Also since our instrument is a scanner the source must emit a constant intensity for throughout the measurement. This may last for several hours.

Microwave discharge tubes are ideally suited for this application, and we have constructed an apparatus for making them. We use the method of Corliss, Bozman and Westfall (1953) to manufacture the tubes, using helium as the buffer gas. In addition to the helium tubes we have successfully made tubes containing helium plus trace amounts of the following substances: (1) hydrogen (2) lithium (3) sodium (4) magnesium (5) calcium (6) mercury and (7) iron. We found that the pure metals reacted slowly with the quartz walls of the tubes when the tubes were at operating temperature 800^{o}K. This shortened their lifetime and made them unstable in their light output. We also experimented with the metal halides, e.g. LiCl, LiBr, CaI_2 etc. We want to find the compounds that give the purest spectra of the metal, and the longest lifetime and stability of the tubes.

We use our instrument to monitor the light output from one of the discharge tubes in the wavelength of the metal line of interest. We have found that the LiBr, Mg and Ca tubes do not give a stable light output with time, and this is due to reactions of these metals with the walls of the chamber.

b) Solar Magnetometer

We have begun testing the magnetic analyzer that was constructed during the last six-month period. We placed the KDP crystal between the entrance pinhole and the collimating mirror, but outside the pressure chamber. Following the KDP crystal is a Glan Thompson prism. The KDP crystal and the Glan Thompson prism can be rotated by 360° independently. Also at the same time a voltage of up to ± 3000 volts can be applied to the KDP crystal. The quarter-wave voltage of this crystal, purchased from ISOMET, is 2000 volts at 5000A. We can vary the voltage anywhere within the ± 3000 volts range within a fraction of a second. The transmission of the KDP crystal plus the Glan Thompson prism for unpolarized light is about 25%.

When we switch the quarter-wave voltage to the KDP crystal from positive to negative polarity we can measure the difference between the right and left-hand circularly polarized components at a given wavelength. We have done this in the violet wing of the iron 5250.2 line in the solar spectrum obtaining 12% intensity difference in the umbral center's spectrum and less than 1% in the normal photosphere. These results compare favorably with those of Livingston (1962). We chose the Fe 5250.2 line for the initial tests because the polarization produced by the atoms radiating this line is insensitive to the field strength provided it exceeds 1000 gauss. This is so except for the smallest umbral center. Thus results on the amount of polarization measured in 5250.2 should not change with spot size and/or field strength, and results obtained with different instruments at different times on different spots can be more easily compared.

One difficulty we found is that the 60A monitor gave a high level of instrumental polarization. This monitor is used to correct for changes in instrumental polarization or light intensity which might be otherwise interpreted as a magnetic field change. We think that the instrumental polarization arises in the curved surface of 1P21 photocell used to monitor this 60A region of the continuum. Since we make a difference measurement of the normal photosphere to spot, this does not make the test results incorrect, but it would increase the error in measuring small magnetic fields as for example in the spot penumbra or for certain bright stars.

We are constructing a light chopper at present that we hope will overcome this difficulty by letting the 60A wide beam and the high resolution beam view the same photocell. The light beams are chopped 20 times a second. In this way the effects of instrumental polarization due to the photocell will be the same for both the high resolution and the 60A wide beam. We will then use the photocell with the lowest level of instrumental polarization to make the measurement.

During the summer several tests on instrumental light scattering were undertaken with Mr. K. Czaja, an undergraduate from Columbia University, under the NSF Undergraduate Research Participation Program. A variety of baffles and occulting mirrors were constructed and tested out, new primary mirrors were used, none of which significantly reduced the observed scattered light levels. We take this to indicate that our low scattered light levels are close to optimal and that a significant fraction thereof is atmospheric in origin. As mentioned in earlier reports, our scattered light readings lie consistently at 0.7% of the disk intensity 1 minute of arc outside the solar limb. This already compares favorably with the experience of Kneer and Mattig (1968) at Capri, who quote mean values of 1.4% and Wittman and Schröter's (1968) results, which implies values of the order of 1% for the Sacramento Peak Observatory.

Papers Presented at Meetings:

1. T. Fay and A. Wyller: "URSIES, an Ultravariable Resolution Single Interferometer Echelle Scanner", presented by Fay at 132 meeting of the American Astromonical Society held in Boulder, Colorado, June 8-11, 1970.
2. T. Fay, A.A. Wyller, H. Yun: "A Study of Strong Lines in Sunspot Umbrae", presented by Yun at 132 meeting of the American Astronomical Society in Boulder, Colorado, June 8-11, 1970.
3. T. Fay and A. Wyller: "A Pressure Scanning Fabry-Perot Spectrometer", presented by Wyller in Commission 9 (Instrumentation) at the Fourteenth General Assembly of the International Astronomical Union held in Brighton, England, August 18-27, 1970.
4. T. Fay and A. Wyller: "Photoelectric Line Profiles in Sunspot Spectra", presented by Wyller in Commission 12 (Solar Radiation) at the Fourteenth General Assembly of the International Astronomical Union, Brighton, England, August 18-27, 1970.
5. T. Fay, R. Hilliard and A. Wyller: "Photoelectric Observations of Stellar Line Profiles", presented by Wyller in Commission 29 (Stellar Spectra) at the Fourteenth General Assembly of the International Astronomical Union, Brighton, England, August 18-27, 1970.

6. T. Fay and A. Wyller: "A Pressure Scanning Fabry-Perot Magnetometer", presented by Wyller at IAU Symposium No. 43 on Solar Magnetic Fields held in Paris, France August 31 - September 4, 1970

<u>Papers published, in press or submitted</u>:

1. "New $C^{13}N^{14}$ Search Regions in the Solar Spectrum", T. Fay and A.A. Wyller, Solar Physics <u>11</u>, 384, 1970.
2. "Precision Constants of the Cyanogen Red System with a Perturbation Analysis", T. Fay, I. Marenin, W. Van Citters, J. Quant. Spect. and Rad. (in press).
3. "Theoretical Models of Sunspots" by H.S. Yun, Ap. J. (in press).
4. " A Magnetostatic Sunspot Model with Twisted Field", H.S. Yun, Accepted for publication in Solar Physics.
5. "A New Empirical Model of a Sunspot Umbra", H.S. Yun, submitted to Solar Physics.

<u>Manuscripts in preparation</u>:

1. "URSIES - an Ultravariable Resolution Single Interferometer Echelle Scanner", by T. Fay and A.A. Wyller, in preparation for submission to Applied Optics.
2. "Photoelectric Line Profiles in Sunspot Umbrae", by T. Fay, A.A. Wyller, for submission to Solar Physics.

References

1. Baranovsky, E.A. and Stepanov, V.E., 1959, Izv. Crim. Astrophys. Obs. 21, 180.

2. Branch, D.R., 1969, "Solar Magnesium Isotopic Abundance Ratios", Ph.D. Thesis, University of Maryland.

3. Brandt, P.N., 1969, Solar Physics 7, 187.

4. Bray, R.J. and Loughhead, R.E., 1965, Sunspots, Barnes and Noble, Inc., p. 31.

5. Corliss, C., Bozman, W., and Westfall, F., 1953, J.O.S.A. 43, 381.

6. David, K.H., 1961, Z. F. Ap. 53, 37.

7. David, K.H., and Elste, G., 1962, Z.F. Ap. 54, 12.

8. Elste, G. 1967, private communication.

9. Fullerton, W. and Elste, G., 1969, Abstract presented at the 131st AAS Meeting in New York.

10. Goldberg, J., Muller, E.A. and Aller, L.H. 1960, Ap. J. Supp. 5, No. 45, 1.

11. Henoux, J.C., 1968, Ann. Ast. 31, 511.

12. Henoux, J.C., 1969, Astron. and Astrophys. 2, 288.

13. Kneer, F. and Mattig, W., 1968, Solar Physics 5, 42.

14. Krishna Swamy, K.S., 1967, Ap. J. 150, 1161.

15. Livingston, W.C., Astronomical Techniques, ed. by W.A. Hiltner, University of Chicago Press 1962, p. 336.

16. Makita, M. 1963, Pub. Astron. Soc. Japan, 15, 145.

17. Mattig, W., 1969, Solar Phys. 6, 413.

18. Pierce, A.K. 1954, Ap. J. 120, 233.

19. Rödberg, H., 1969, Nature 221, 394.

20. Schlüter, A. and Temesvary, S. 1958, Electromagnetic Phenomena in Cosmical Physics, Symp. I.A.U., No. 6, 263.

21. Wittmann, A. and Schröter, E.H., 1969, Solar Physics 10, 357.

22. Yun, H.S., 1968, "Theoretical Sunspot Models" Ph.D. Thesis, Indiana University.

23. Zwaan, C. 1965a, Sunspot Models, Recherches Astronomique de l'observatoire d'Utrecht, XVII (4).

24. Zwaan, C. 1965b, The Solar Spectrum, ed. C.de Jager, p. 262.

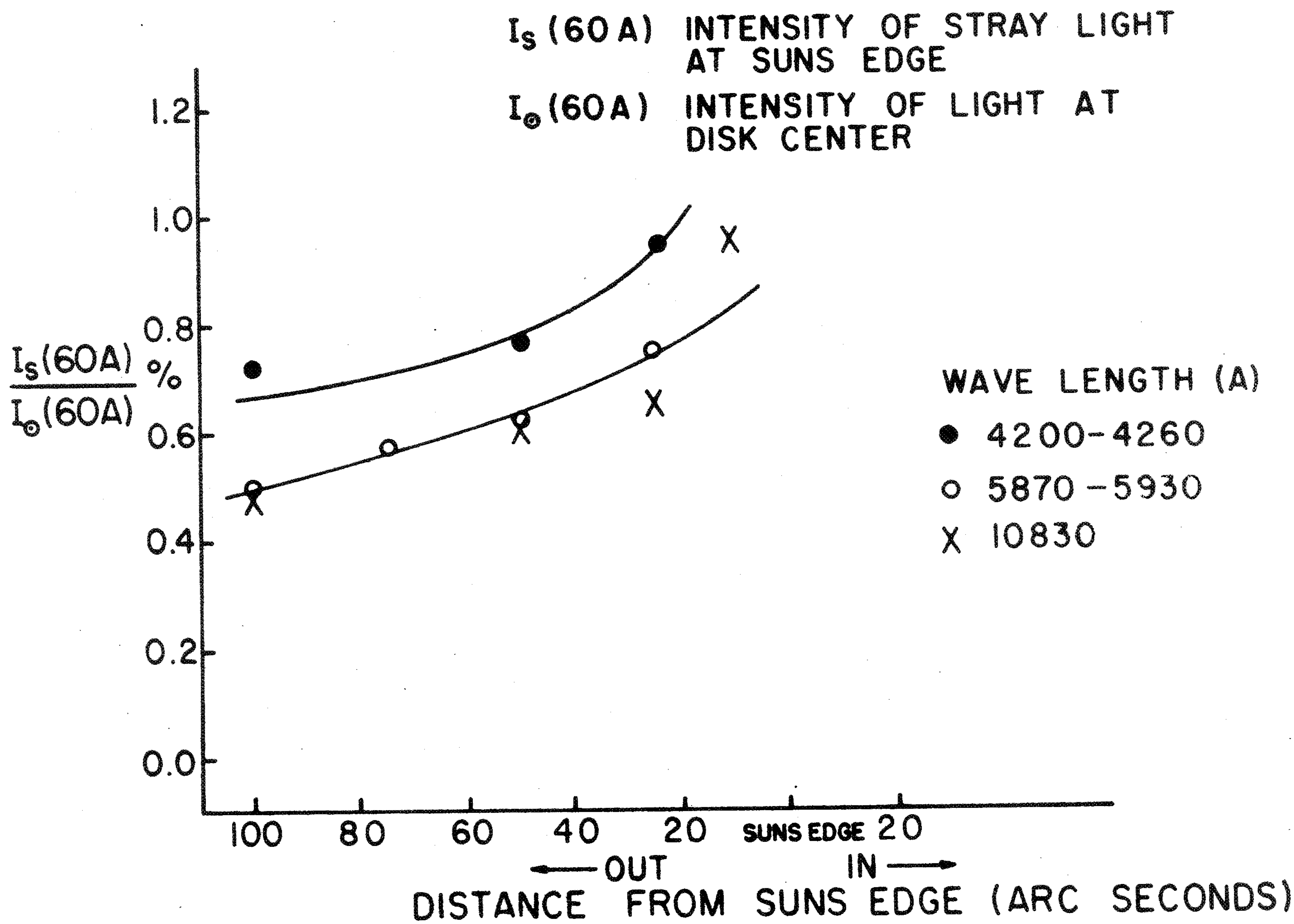

Is (60 A) INTENSITY OF STRAY LIGHT AT SUNS EDGE
I⊙ (60 A) INTENSITY OF LIGHT AT DISK CENTER
1.2
1.0
0.8
0.6
0.4
0.2
0.0
Is(60A) / I⊙(60A) %
WAVE LENGTH (A)
4200-4260
5870-5930
X 10830
100
80
60
40
20
SUNS EDGE
20
OUT
IN
DISTANCE FROM SUNS EDGE (ARC SECONDS)

Fig. 1

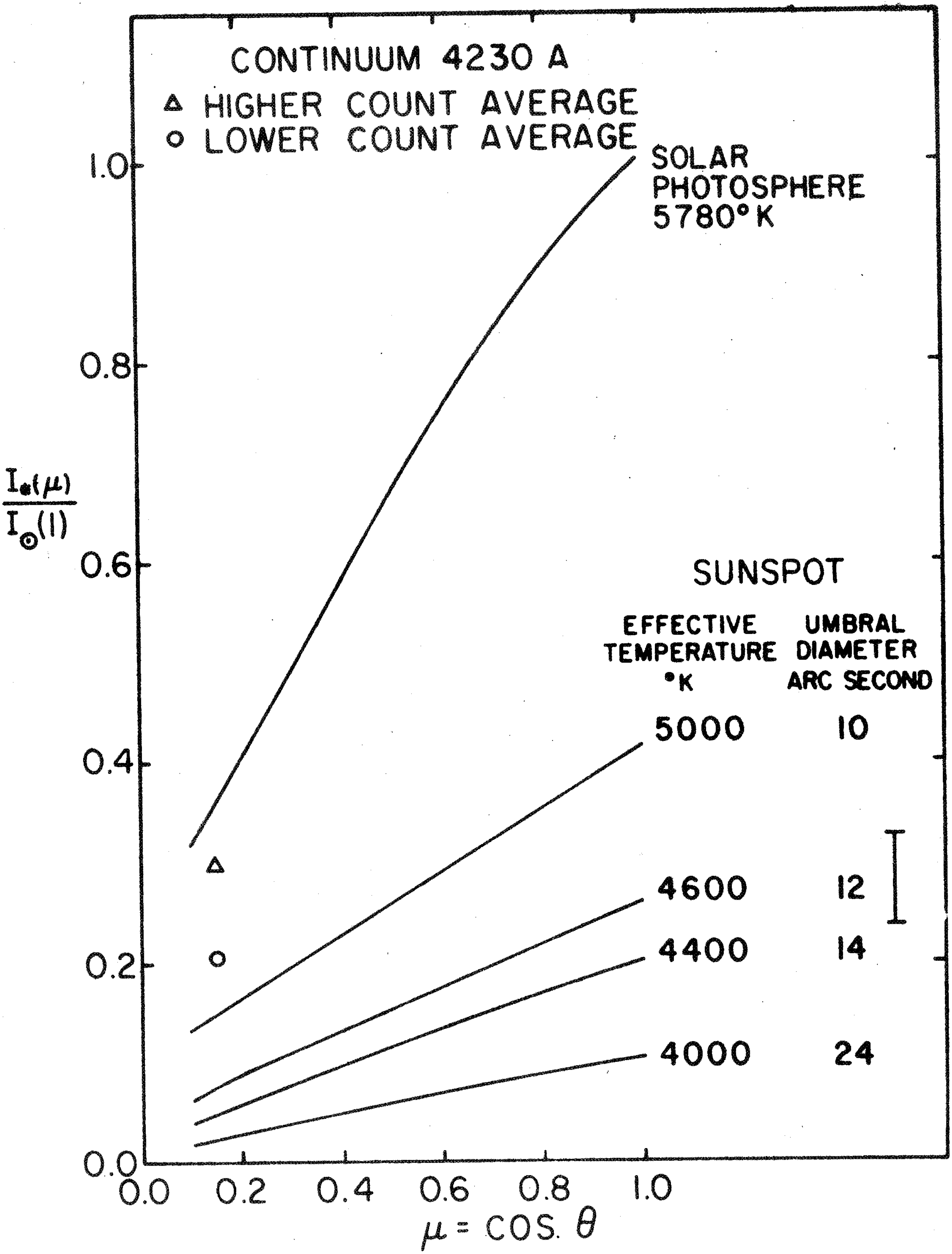

CONTINUUM 4230 A
HIGHER COUNT AVERAGE
LOWER COUNT AVERAGE
SOLAR PHOTOSPHERE 5780°K
SUNSPOT
EFFECTIVE TEMPERATURE °K
UMBRAL DIAMETER ARC SECOND
5000
10
4600
12
4400
14
4000
24
1.0
0.8
0.6
0.4
0.2
0.0
0.0
0.2
0.4
0.6
0.8
1.0
μ = COS. θ

Fig. 2

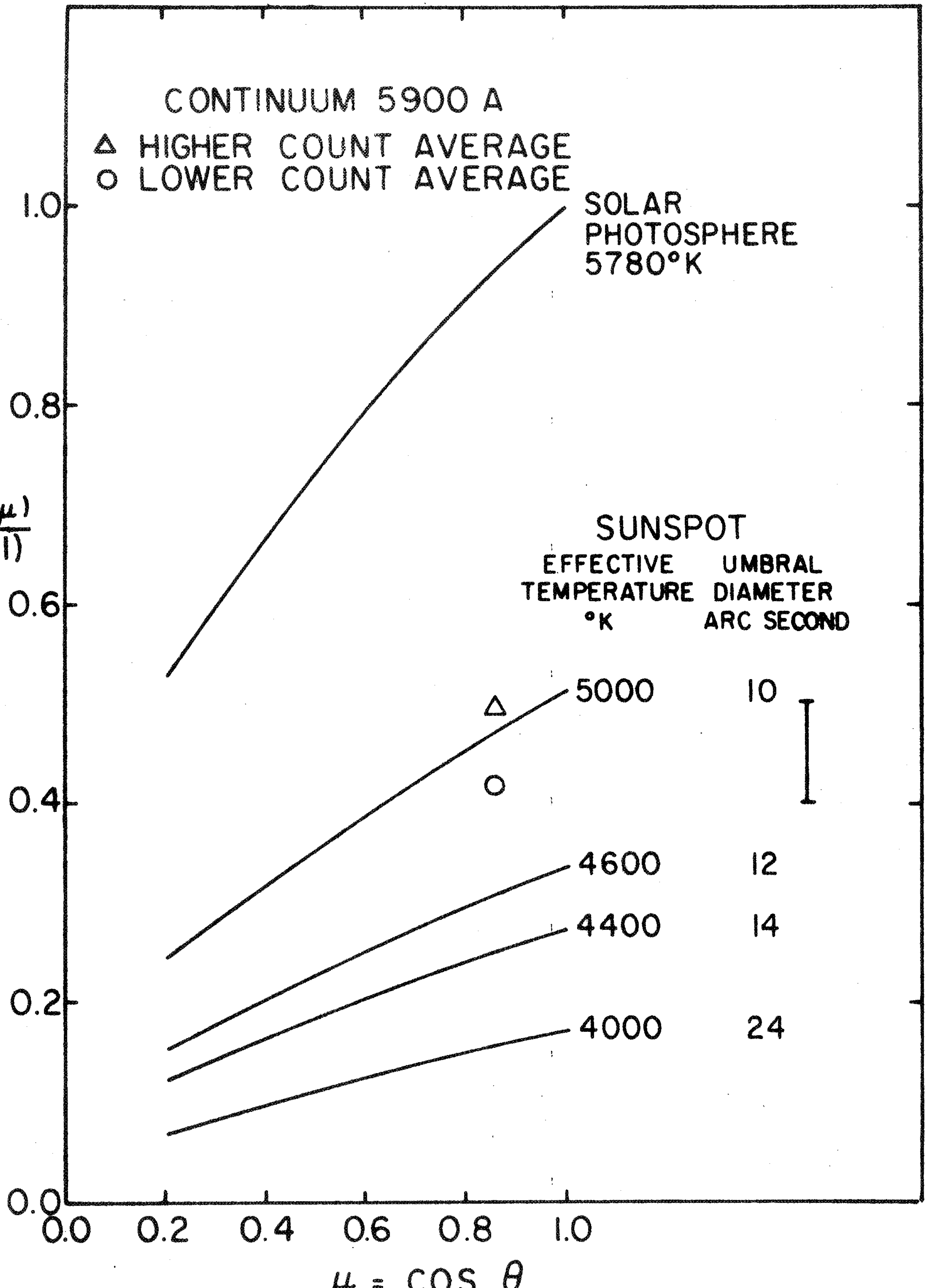

CONTINUUM 5900 A
△ HIGHER COUNT AVERAGE
○ LOWER COUNT AVERAGE
SOLAR PHOTOSPHERE 5780°K
SUNSPOT
EFFECTIVE TEMPERATURE °K
UMBRAL DIAMETER ARC SECOND
5000 10
4600 12
4400 14
4000 24
$\frac{I_*(\mu)}{I_\odot(1)}$
1.0
0.8
0.6
0.4
0.2
0.0
0.0 0.2 0.4 0.6 0.8 1.0
$\mu = \cos\theta$

Fig. 3

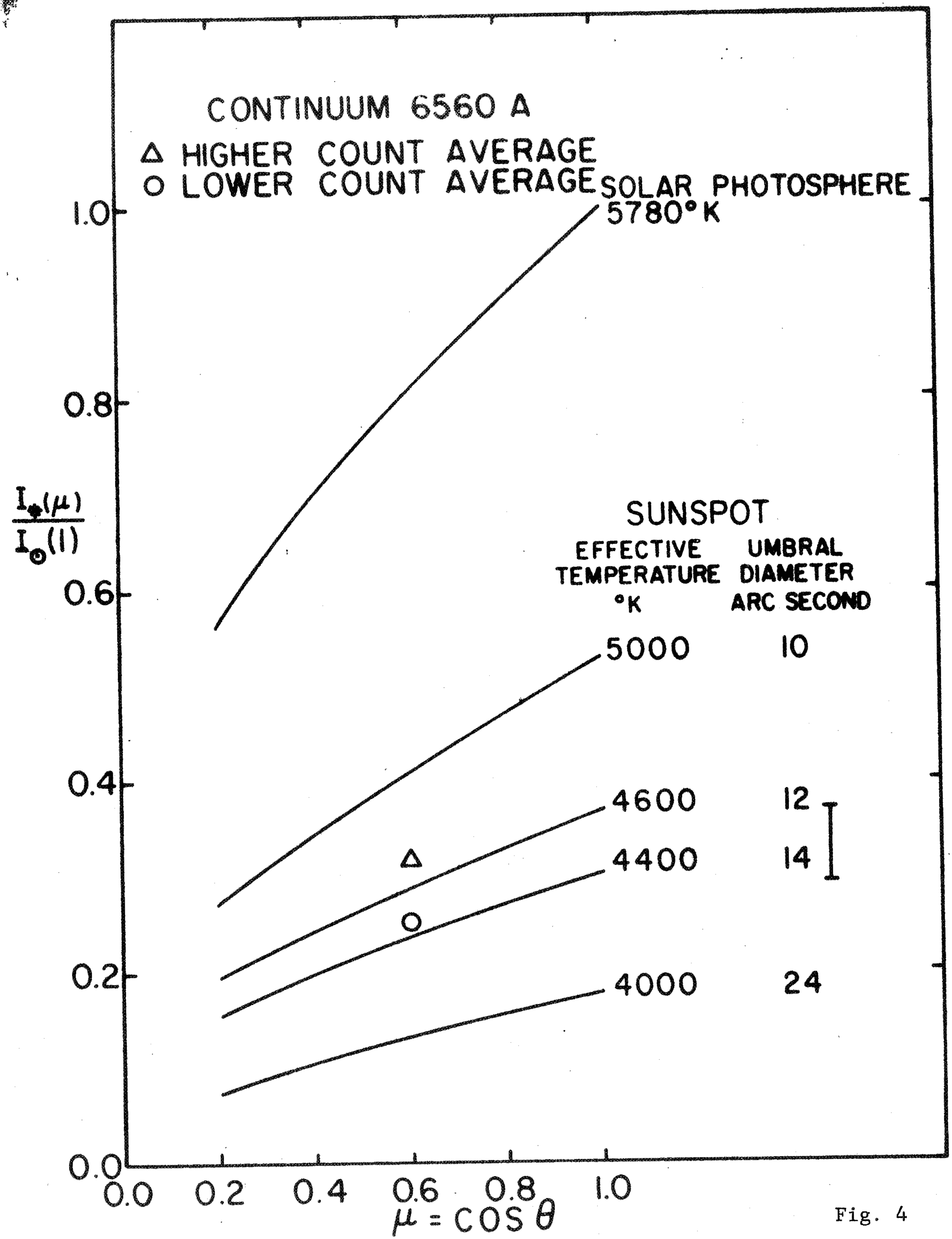

CONTINUUM 6560 A
△ HIGHER COUNT AVERAGE
○ LOWER COUNT AVERAGE
SOLAR PHOTOSPHERE
5780°K
SUNSPOT
EFFECTIVE TEMPERATURE °K
UMBRAL DIAMETER ARC SECOND
5000
10
4600
12
4400
14
4000
24
1.0
0.8
0.6
0.4
0.2
0.0
0.0
0.2
0.4
0.6
0.8
1.0
$\frac{I_*(\mu)}{I_\odot(1)}$
$\mu = \cos\theta$

Fig. 4

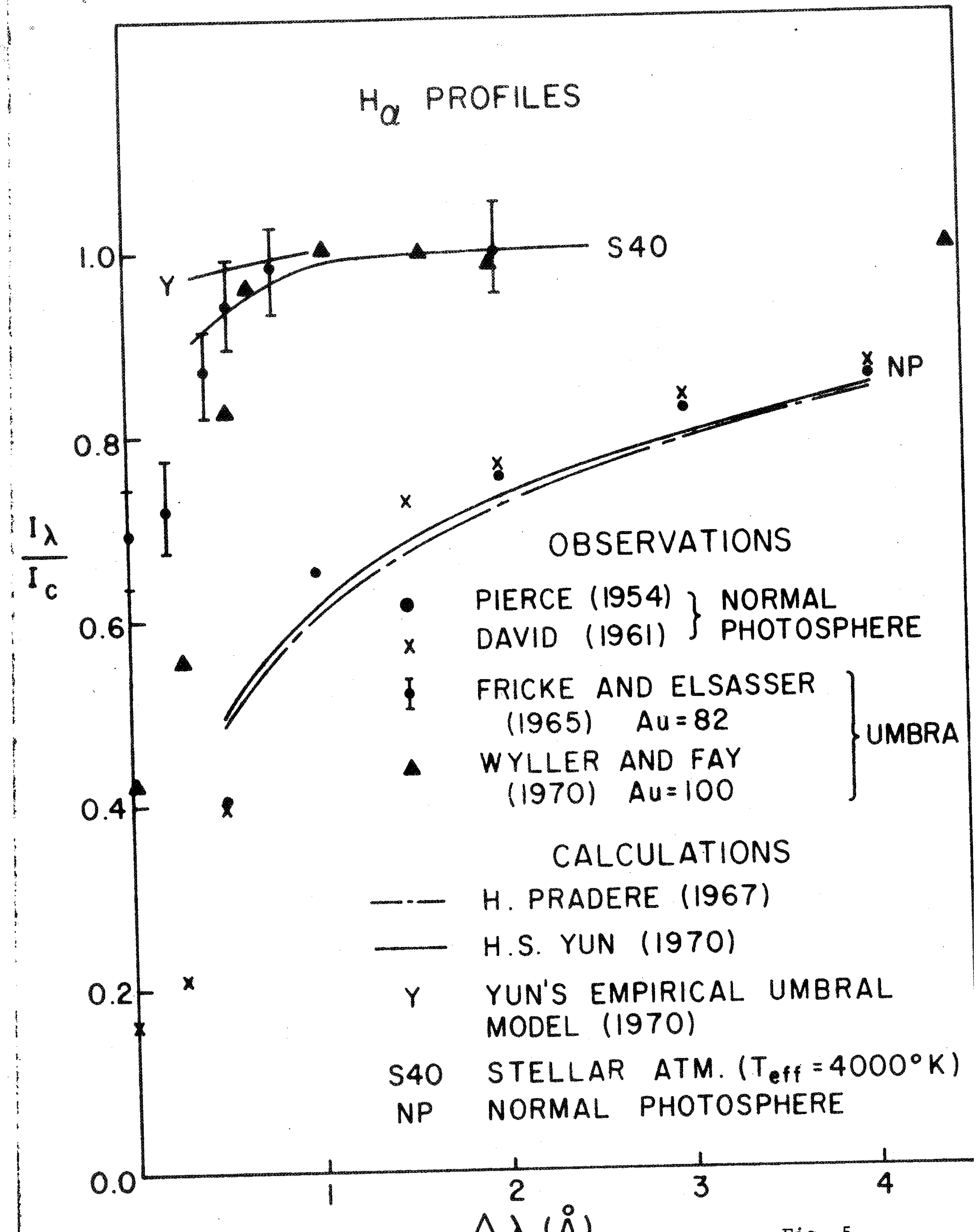

H$_\alpha$ PROFILES
S40
Y
NP
I_λ / I_c
1.0
0.8
0.6
0.4
0.2
0.0
1
2
3
4
$\Delta\lambda$ (Å)
OBSERVATIONS
PIERCE (1954) } NORMAL PHOTOSPHERE
DAVID (1961)
FRICKE AND ELSASSER (1965) Au=82 } UMBRA
WYLLER AND FAY (1970) Au=100
CALCULATIONS
H. PRADERE (1967)
H.S. YUN (1970)
Y YUN'S EMPIRICAL UMBRAL MODEL (1970)
S40 STELLAR ATM. (T_{eff} = 4000°K)
NP NORMAL PHOTOSPHERE

Fig. 5

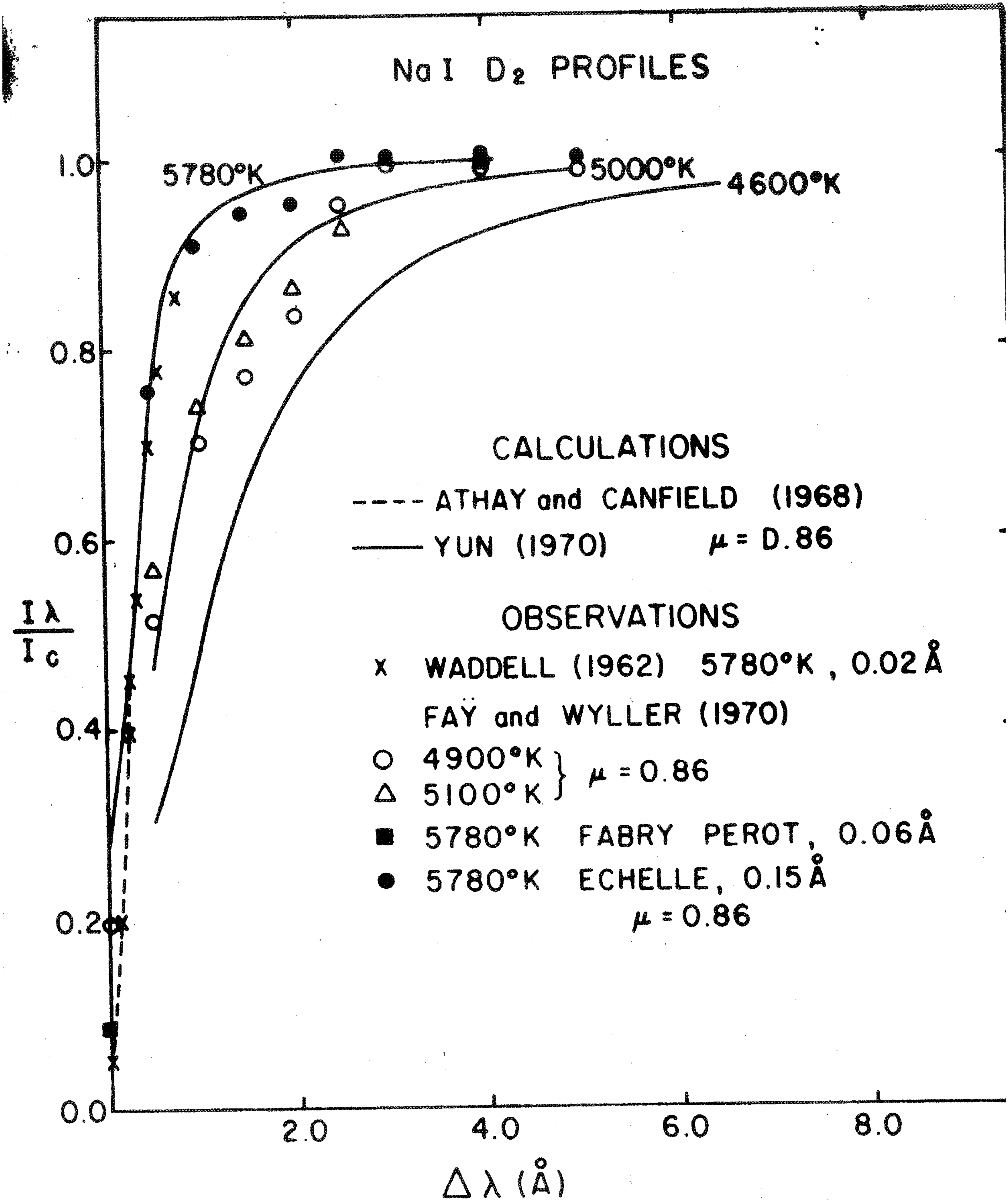
Na I D2 PROFILES
5780°K
5000°K
4600°K
CALCULATIONS
---- ATHAY and CANFIELD (1968)
—— YUN (1970) μ = D.86
OBSERVATIONS
x WADDELL (1962) 5780°K, 0.02 Å
FAŸ and WYLLER (1970)
○ 4900°K
△ 5100°K
μ = 0.86
■ 5780°K FABRY PEROT, 0.06 Å
● 5780°K ECHELLE, 0.15 Å
μ = 0.86
Iλ / Ic
0.0
0.2
0.4
0.6
0.8
1.0
2.0
4.0
6.0
8.0
Δλ (Å)

Fig. 6

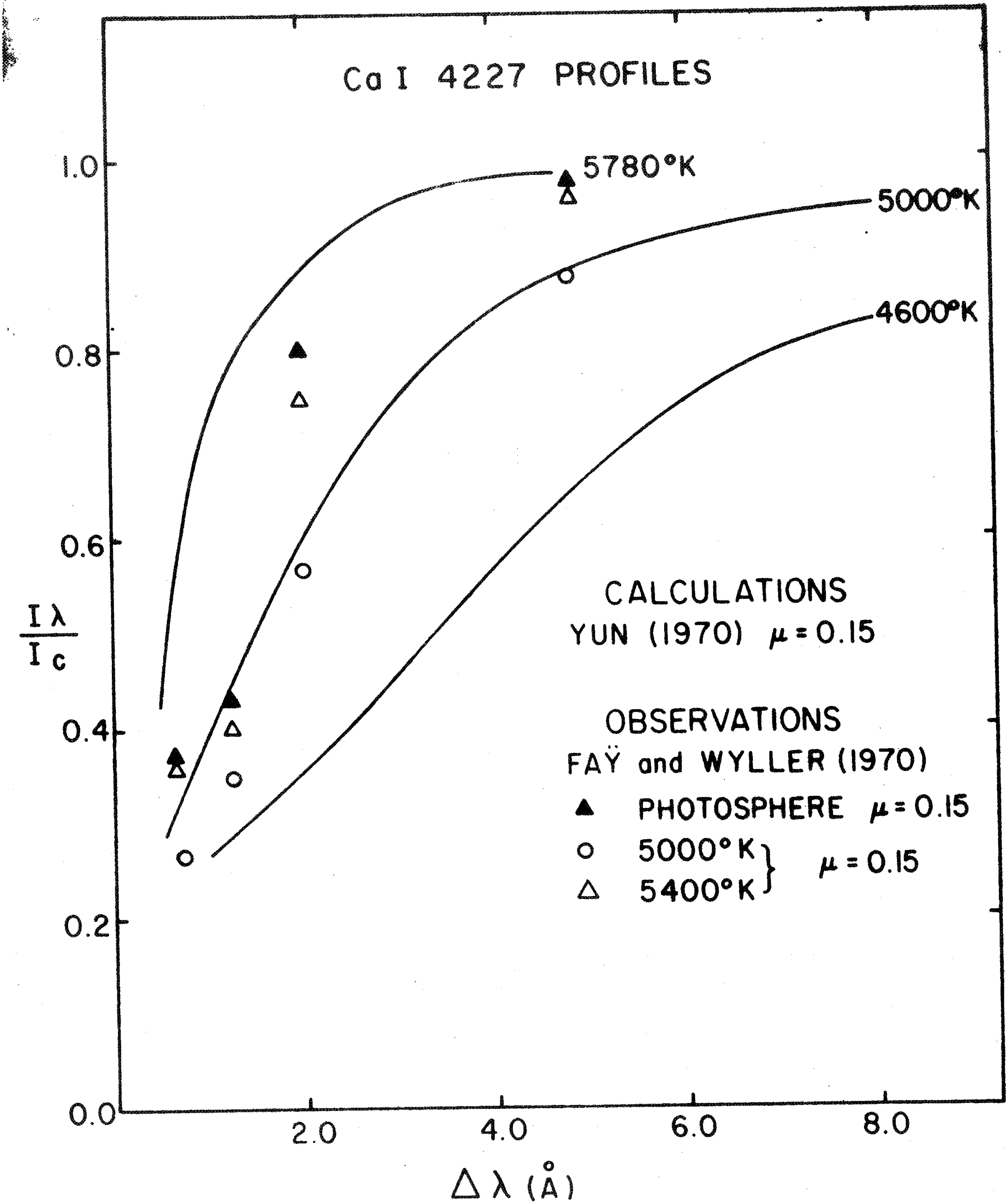
Ca I 4227 PROFILES
5780°K
5000°K
4600°K
CALCULATIONS
YUN (1970) μ = 0.15
OBSERVATIONS
FAŸ and WYLLER (1970)
PHOTOSPHERE μ = 0.15
5000°K
5400°K
μ = 0.15
1.0
0.8
0.6
0.4
0.2
0.0
Iλ / Ic
2.0
4.0
6.0
8.0
Δλ (Å)

Fig. 7

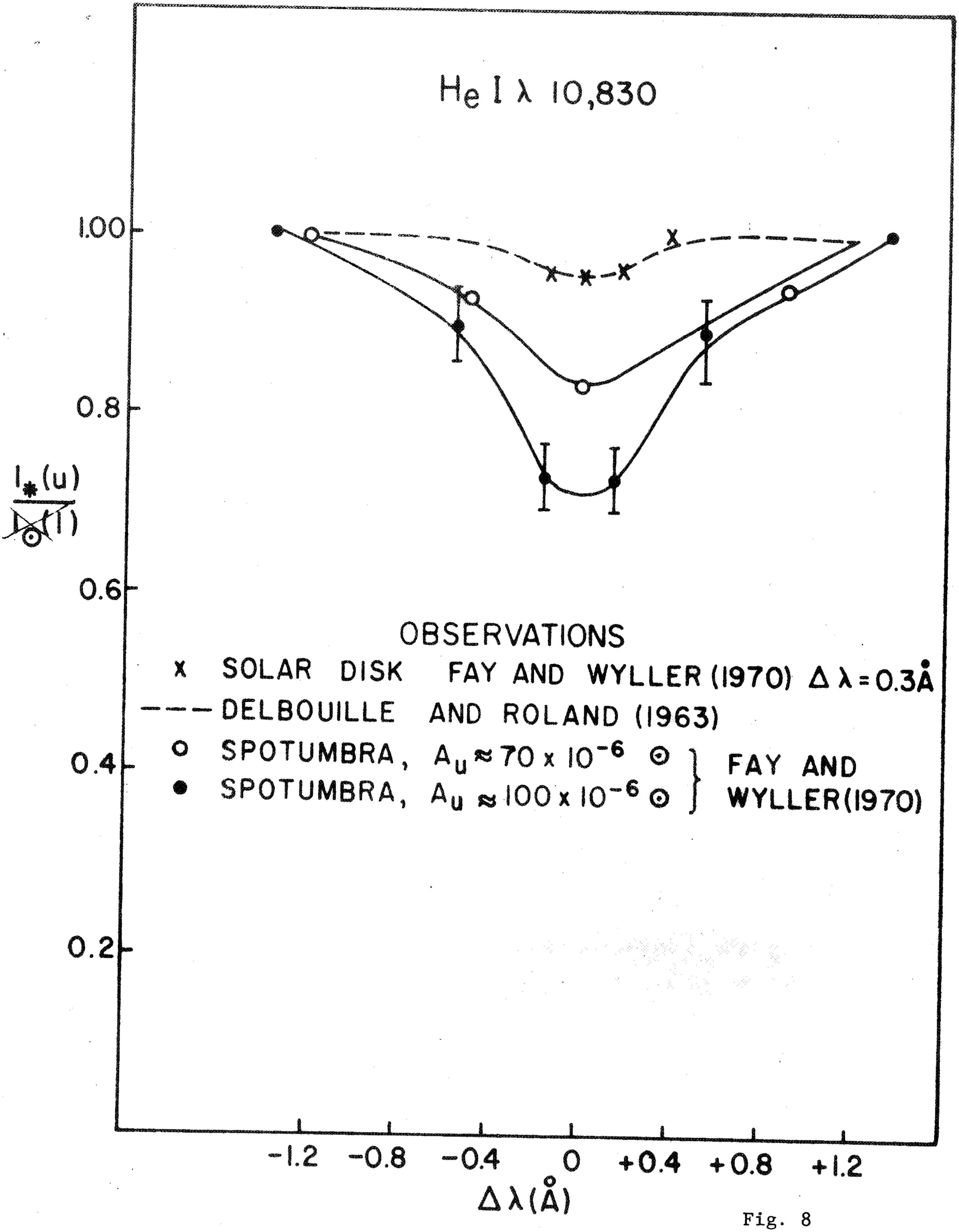

He I λ 10,830
1.00
0.8
0.6
0.4
0.2
I*(u) / I⊙(1)
-1.2
-0.8
-0.4
0
+0.4
+0.8
+1.2
Δλ(Å)
OBSERVATIONS
x SOLAR DISK FAY AND WYLLER (1970) Δλ = 0.3Å
DELBOUILLE AND ROLAND (1963)
SPOTUMBRA, Au ≈ 70 x 10-6 ⊙
SPOTUMBRA, Au ≈ 100 x 10-6 ⊙
FAY AND WYLLER(1970)

Fig. 8

Figure Captions

Figure 9 Observed and computed center-to-limb variations of the intensity ratio $\phi_\lambda(u) = I^*_\lambda(u)/I^\odot_\lambda(u)$. The solid lines in Figures a, b and c refer to the computed intensity ratio as each specified wavelength based on the new empirical model (i.e. YN - Yun's model). Other umbral models considered in the calculation are MT - Makita (1963), ZW - Zwaan (1965), HX - Henous (1969), WS - Wittmann and Schröter (1969) and S40 - Scaled solar model of T^*_{eff}=4000°K.

Figure 10a $T - \tau_0$ relations of different empirical umbral models. BR refers to Branch's model (1969). The symbols representing other umbral models are the same as in Figure 1.

Figure 10b Observed and computed profiles of Na I D_2 lines. The observed profiles are given by Baranovsky and Stepanov (1959) (○). Henoux (1969) (▲) and by Fay and Wyller (1970) (● for the umbra and x for the normal photosphere). The computed profiles from a solar model atmosphere by Gingerich (1970) and four different empirical umbral models are given (see Figure 1 for the symbols representing the umbral models).

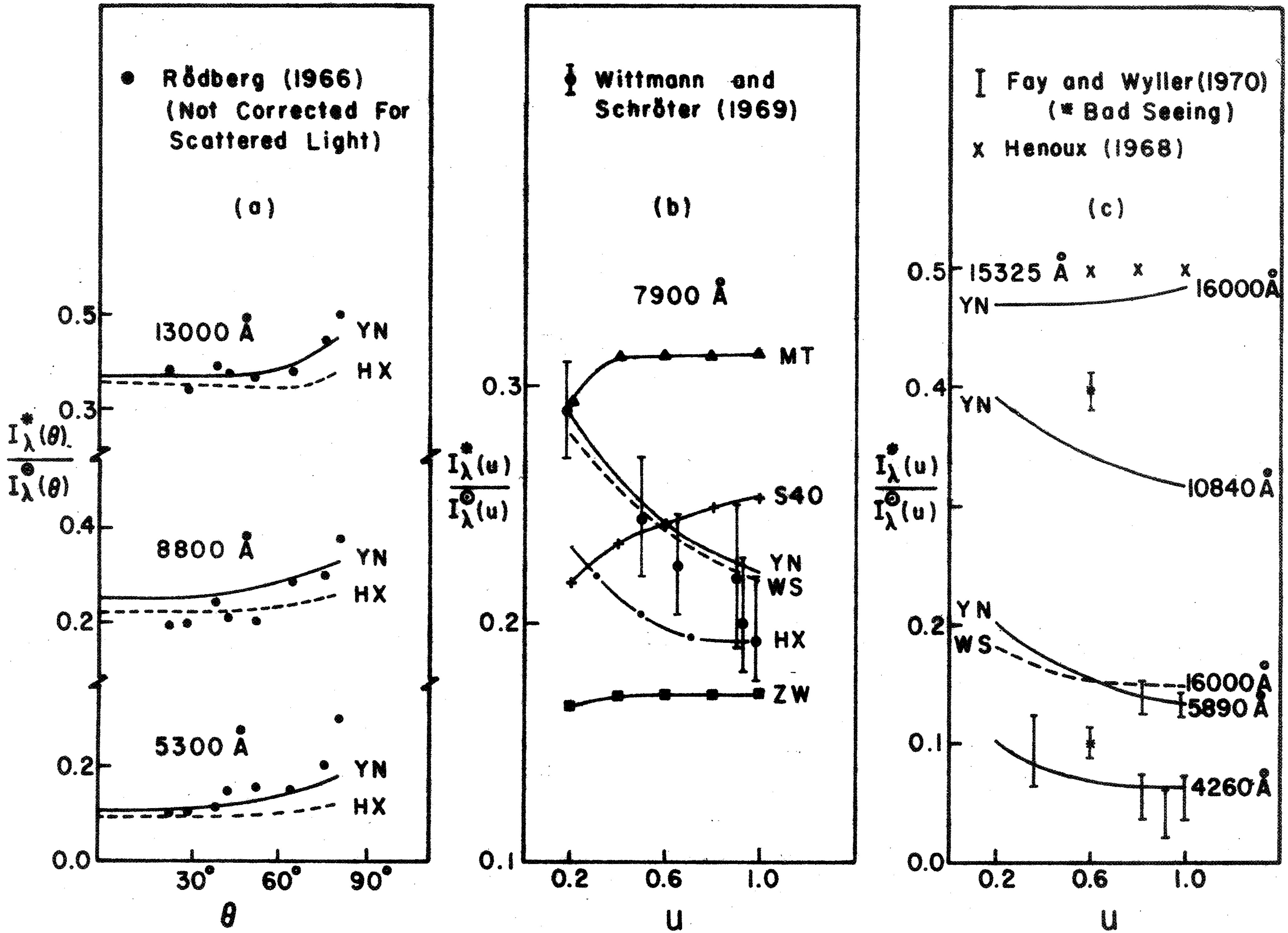

Rödberg (1966)
(Not Corrected For
Scattered Light)
(a)
13000 Å
YN
HX
8800 Å
YN
HX
5300 Å
YN
HX
$I_\lambda^*(\theta) / I_\lambda^\odot(\theta)$
0.5
0.3
0.4
0.2
0.2
0.0
30°
60°
90°
θ
Wittmann and
Schröter (1969)
(b)
7900 Å
MT
S40
YN
WS
HX
ZW
$I_\lambda^*(u) / I_\lambda^\odot(u)$
0.3
0.2
0.1
0.2
0.6
1.0
u
Fay and Wyller (1970)
(* Bad Seeing)
x Henoux (1968)
(c)
15325 Å
16000 Å
YN
YN
10840 Å
YN
WS
16000 Å
5890 Å
4260 Å
$I_\lambda^*(u) / I_\lambda^\odot(u)$
0.5
0.4
0.2
0.1
0.0
0.2
0.6
1.0
u

Fig. 9

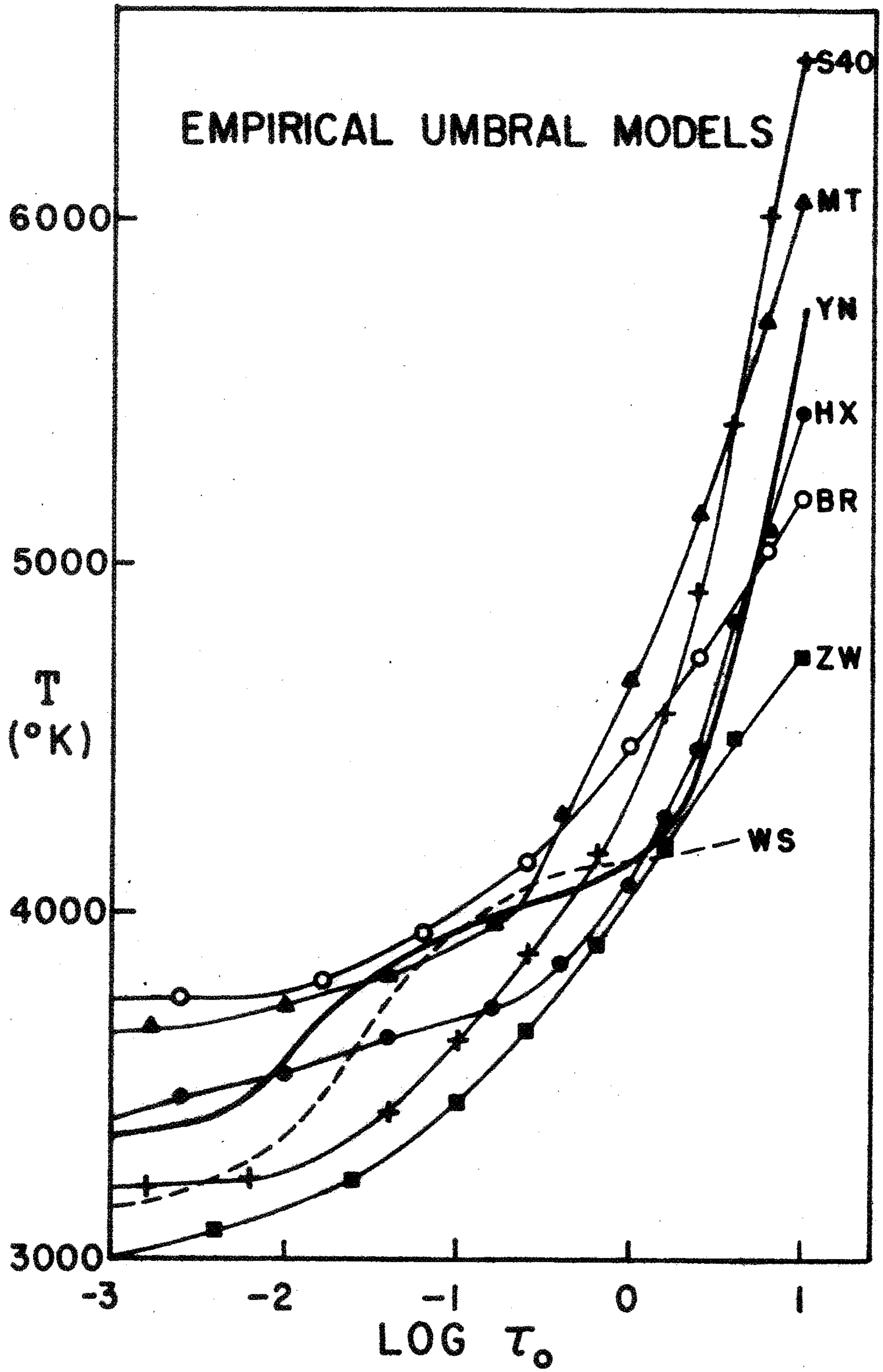

Fig. 10a

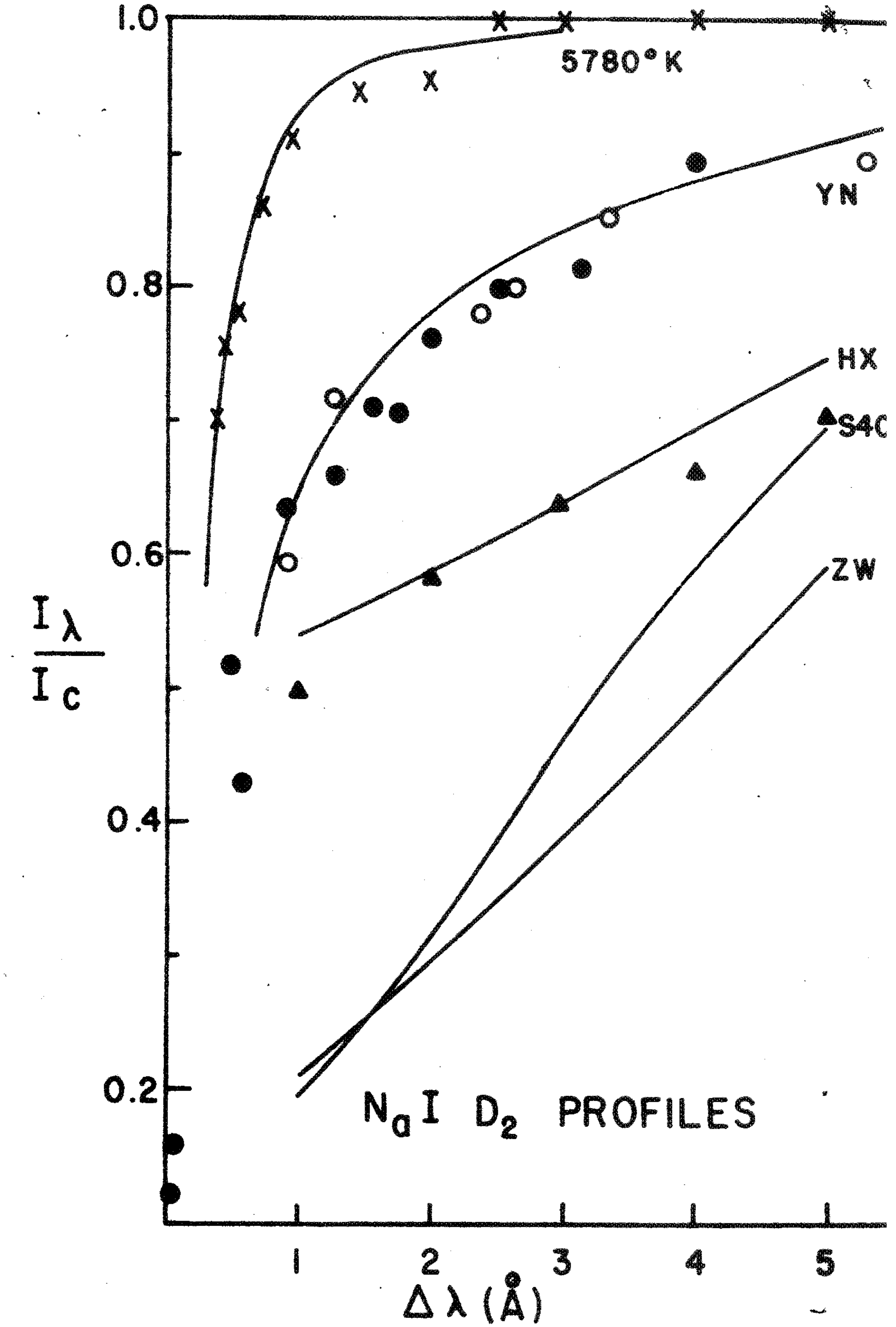

Fig. 10b